ENSO and Hydrologic Extremes in the Western United States*

DANIEL R. CAYAN

Climate Research Division, Scripps Institution of Oceanography, and U.S. Geological Survey, La Jolla, California

KELLY T. REDMOND

Western Regional Climate Center, Reno, Nevada

LAURENCE G. RIDDLE

Climate Research Division, Scripps Institution of Oceanography, La Jolla, California

(Manuscript received 14 August 1998, in final form 1 December 1998)

ABSTRACT

Frequency distributions of daily precipitation in winter and daily stream flow from late winter to early summer, at several hundred sites in the western United States, exhibit strong and systematic responses to the two phases of ENSO. Most of the stream flows considered are driven by snowmelt. The Southern Oscillation index (SOI) is used as the ENSO phase indicator. Both modest (median) and larger (90th percentile) events were considered. In years with negative SOI values (El Niño), days with high daily precipitation and stream flow are more frequent than average over the Southwest and less frequent over the Northwest. During years with positive SOI values (La Niña), a nearly opposite pattern is seen. A more pronounced increase is seen in the number of days exceeding climatological 90th percentile values than in the number exceeding climatological 50th percentile values, for both precipitation and stream flow. Stream flow responses to ENSO extremes are accentuated over precipitation responses. Evidence suggests that the mechanism for this amplification involves ENSO-phase differences in the persistence and duration of wet episodes, affecting the efficiency of the process by which precipitation is converted to runoff. The SOI leads the precipitation events by several months, and hydrologic lags (mostly through snowmelt) delay the stream flow response by several more months. The combined 6–12-month predictive aspect of this relationship should be of significant benefit in responding to flood (or drought) risk and in improving overall water management in the western states.

1. Introduction

One of the few relatively reliable predictive links to anomalous precipitation in North America on seasonal timescales involves the connection to large-scale disturbed conditions in the tropical Pacific, known as the El Niño–Southern Oscillation (ENSO) phenomenon (Rasmusson and Carpenter 1982; Rasmusson and Wallace 1983). Though the ENSO connection to precipitation fluctuations in western North America is weaker than that in some other regions around the globe, a number of studies have established that western North America contains a significant ENSO signal in precipitation, snow accumulation, and stream flow (e.g., Andrade and Sellers 1988; Yarnal and Diaz 1986; Kiladis and Diaz 1989; Cayan and Peterson 1989; Schonher and Nicholson 1989; Redmond and Koch 1991; Cayan and Webb 1992; Cayan 1996; Kahya and Dracup 1993, 1994; Dracup and Kahya 1994; Livezey et al. 1997; Piechota et al. 1997; Dettinger et al. 1998, 1999). Besides having a well-established link between western precipitation and the tropical Pacific when it is in its warm (El Niño) phase, there is solid evidence for an analogous link to the cool (La Niña) phase (Redmond and Koch 1991; Redmond and Cayan 1994; Dracup and Kahya 1994; Kahya and Dracup 1994; Livezey et al. 1997). These analyses show a decided pattern of opposite association with the ENSO phase, such that the Southwest tends to be wet and the Northwest dry during El Niño (negative Southern Oscillation index), and vice versa for La Niña (positive Southern Oscillation index). In addition, the consistency of the relationship appears to be greater for the positive Southern Oscillation index (SOI) than for the negative SOI, a facet that has not been widely appreciated (see Redmond and Cayan 1994).

* WHOI Contribution Number 9971.

Corresponding author address: Dr. Daniel R. Cayan, Climate Research Division, Scripps Institution of Oceanography, 9500 Gilman Drive, Dept. 0224, La Jolla, CA 92093-0224.
E-mail: dcayan@ucsd.edu

The ''centers of action'' of this opposition pattern appear to lie near the southern and northern U.S. borders (Dettinger et al. 1998). About half the flow of the Columbia River measured at The Dalles (Oregon) originates in British Columbia, and the spring–summer stream flow at this point is well correlated with the phase of ENSO (Pulwarty and Redmond 1997). Shabbar et al. (1997) show a dry maximum in El Niño years, and a wet maximum in La Niña years, for winter precipitation centered over the headwaters region of the Columbia. For southern Canada, they also show that this relationship extends over the entire winter snowpack accumulation season. This same opposition pattern prompted Redmond and Koch (1991) to aggregate the six coolest months in analyzing impacts of ENSO on surface climate variability over the western United States. Also, the principal audience (water managers) for this information is less interested in the detailed evolution of how the winter snowpack is laid down and more interested in what the final premelt snowpack status is at the beginning of April.

The studies cited above examined the link between ENSO and seasonal aggregations of quantities such as temperature, precipitation, snowfall, or river discharge. However, it is clear that both daily precipitation amounts and precipitation frequencies are affected by ENSO events (Cayan and Webb 1992; Woolhiser et al. 1993; Gershunov and Barnett 1998). The present study is distinguished from these others in that it takes a comprehensive analysis of how precipitation and the resultant land surface runoff (represented by stream flow records) respond together to ENSO. Also, there is intriguing evidence of low-frequency changes (even trends) in the occurrence of daily precipitation as well as in the intensity of larger daily precipitation events across much of the United States (Karl and Knight 1998); it is quite possible that trends and regimes in ENSO contribute to a portion of this kind of variability. Thus, an important question concerns how the number and nature of events from a spatially comprehensive set of daily hydrologic records, such as for the western United States, are affected by ENSO.

Although by far the most frequent daily precipitation totals are very light (e.g., 2 mm day^{-1} or less), the contribution to the total seasonal water volume from the heavier (25 mm day^{-1} and greater) precipitation totals is very substantial. Climatological statistics for Nevada City, California (Fig. 1), show the frequency distribution of October–March daily precipitation amounts and their contribution to the total seasonal volume, illustrating the crucial role of heavy precipitation events. Woodhouse and Meko (1997) have found that natural recorders of climate, such as tree rings, may respond more to precipitation frequency than to its total accumulated amount. Other studies have established that ENSO conditions can also be associated with shifts in the frequency of precipitation events of various magnitudes (Woolhiser et al. 1993; Cayan and Webb 1992). For

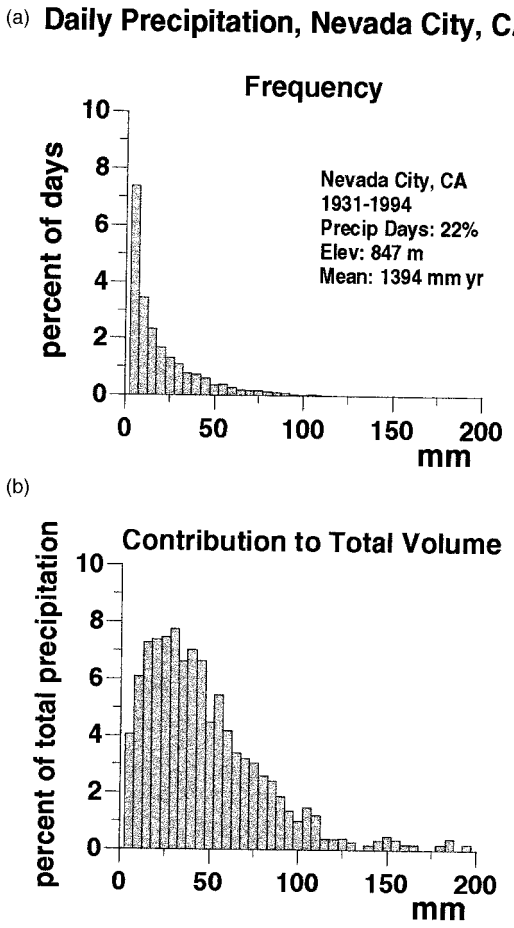

FIG. 1. Daily precipitation amounts, Nevada City, CA, Oct–Apr, 1931–95. Frequency distribution, expressed as (a) percent of total days (wet and dry days) and (b) contribution to total precipitation volume within period.

example, heavy precipitation events (>90th percentile) in San Diego, California (Fig. 2), are more likely during El Niño winters than during La Niña. Figure 2 shows that 12 of the 21 El Niño winters since 1931 have produced above-normal numbers (more than 5 days per winter) of heavy precipitation days; only 3 of 12 La Niña winters have produced above-normal numbers, half of these winters had less than 4, and 3 of them had zero days with heavy precipitation.

The current study examines daily precipitation occurrences over the western conterminous United States to determine how ENSO events have influenced the frequency of occurrence of different daily amounts, especially the high extremes. Because stream flow often responds dramatically to heavy precipitation events, and even more to frequent heavy precipitation events, we also evaluate frequencies of stream flow rates. These ENSO-influenced stream flow events corroborate the ENSO influence upon precipitation events and are of considerable practical importance in themselves. In this paper ''extreme'' is referenced to station-specific sta-

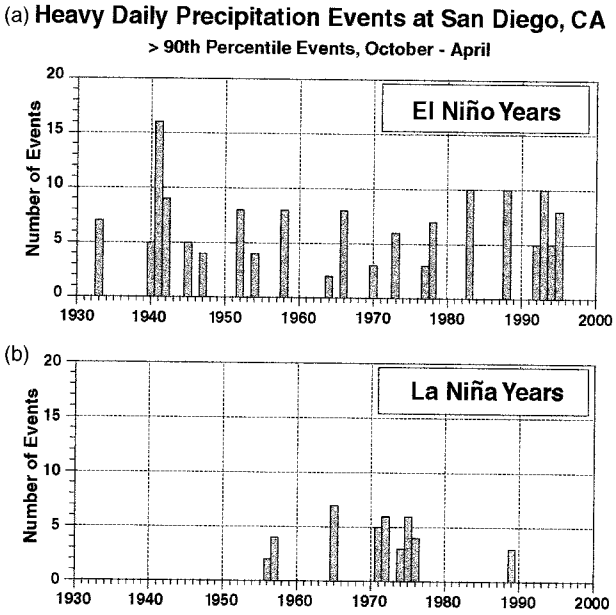

FIG. 2. Number of days with precipitation exceeding daily 90th percentile in SOI− (El Niño) and SOI+ (La Niña) years, San Diego, CA, Oct–Apr, 1931–95. Approximately six P90 events per year are expected, on average, over the entire record.

tistics derived from daily observations (both precipitation and stream flow) for the period 1948–95. Following earlier studies (Redmond and Koch 1991; Redmond and Cayan 1994), we define the ENSO state by using a simple average of the Southern Oscillation index during boreal summer and fall (rationale below) and consider the precipitation and stream flow in the subsequent winter through summer period. Thus, these analyses constitute a test of the predictive power of ENSO upon hydrologic extremes over the region at seasonal time leads.

2. Data

The area covered in this study encompasses the 11 mountainous states in the western conterminous United States, from Montana south to New Mexico and then west to the Pacific Ocean. The period covered primarily is 1948–95, although longer records are included for a few specific sites. The precipitation dataset consists of daily rain gauge observations compiled by the National Climate Data Center (NCDC) from 293 first-order and cooperative stations, each having a relatively long and complete period of record (Fig. 3a). For the interval 1948–95, 92% of the stations have less than 5% missing data, 97% have less than 10% missing, and only one station has more than 20% missing data. At a few stations where individual analyses were conducted, longer periods of record (as early as 1931 and as late as 1997) were employed. This paper examines precipitation only during the cool season (October–April), when the bulk of the west's precipitation falls, especially in its mountains, to become the source of most stream flow (Farnes 1995).

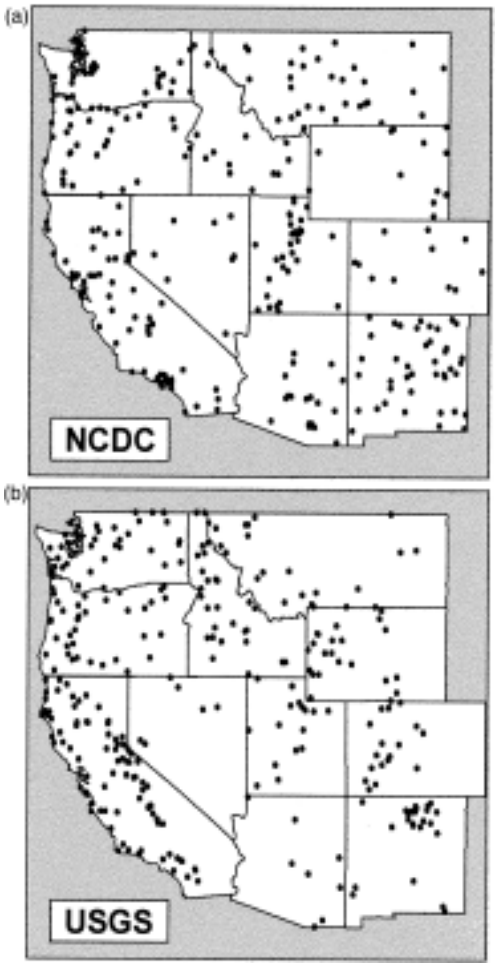

FIG. 3. Areal distribution of selected (a) NCDC precipitation stations and of (b) USGS stream gauges.

The stream flow dataset consists of the daily mean observations from 303 U.S. Geological Survey (USGS) gauging stations (Fig. 3b). The stream flow gauges selected are from the compilation of Slack and Landwehr (1992), considered by them to have been minimally affected by artificial influences such as upstream water storage and diversion, water use practices, and land use changes. These records, for the period 1948–89, were extended through 1995 at gauges where daily mean stream flow data were readily available from the USGS database. The median drainage area for the 303 gauging stations is 78.5 km^2, with over 90% of the drainage being less than 3000 km^2 and the largest, 10 230 km^2. For the interval 1948–95, 30% of the stream flow records have less than 5% missing data, 49% have less than 10% missing, and 76% have less than 20% missing. The main reason for missing stream flow data is that the individual station records began after 1948 or ended prior to 1995. Most of our focus is upon stream flow

during winter through early summer (January–July), when most of the annual runoff in the west occurs (Cayan and Peterson 1989).

The ENSO state is represented by the SOI, defined as the standardized difference in sea level pressure anomalies, Tahiti minus Darwin, Australia (Ropelewski and Jones 1987). Monthly SOI updates were obtained from the National Oceanic and Atmospheric Administration Climate Prediction Center. Following Redmond and Koch (1991) we use the average SOI for June–November preceding the winter in question. Correlations with SOI leading climate by a few months are slightly higher or equal to simultaneous correlations, allowing the possibility of predictive relationships (see also a further discussion of predictions of stream flow by Kahya and Dracup 1994). When the June–November average SOI is −0.50 or less (hereafter ''SOI−''), the tropical Pacific is most likely to be in its warm (El Niño) phase. When it averages +0.50 or greater (hereafter ''SOI+''), the tropical Pacific is most likely in its cool (La Niña) phase. About half the years fit either one or the other of these criteria. The in-between case is labeled ''neutral.'' Other measures of ENSO are often used. In particular, sea surface temperature is often employed because of the belief that it is the driving physical variable. Recently, Wolter and Timlin (1998) have introduced the ''Multivariate ENSO Index,'' and other measures have been proposed; for example, Harrison and Larkin (1998) discuss such patterns. However, the goal here is threefold: to use a measure that 1) adequately (if not optimally) serves as an indicator of ENSO status, 2) correlates well with western North America climate and stream flow, and 3) maintains a good relationship to climate at lead times of at least several months. For our purposes, an index that can act as a surrogate for perhaps more ''physical'' quantifies is sufficient, and the readily available SOI serves well on all three criteria.

3. Methodology

a. Percentiles

Daily data from 1948–55 were used to estimate precipitation and stream flow percentiles (10th, 25th, 50th, 75th, and 90th) for each day of the year at each station (Fig. 3). For precipitation, percentiles were estimated only for nonzero values; dry days were excluded. For each day of the year at each station, these statistics were estimated from a sequence of days within a sliding 15-day window centered on that particular day. Each of the above percentiles was determined from the empirical distributions consisting of daily values drawn from all available years and all available dates within the sliding window. This window is long enough to increase the sample size and smooth the resulting values, and yet short enough to permit the values to closely track the seasonal cycle. To further reduce day-to-day fluctuations, values were subsequently smoothed with a 31-day centered Gaussian filter.

Most locations in the western United States contain a marked annual cycle in each of the percentiles. As shown in the central Sierra Nevada region (Fig. 4), precipitation at Nevada City, California, displays a pronounced Mediterranean-type winter maximum and summer minimum. There is an even more marked annual cycle in stream flow at the nearby Merced River (Happy Isles gauge), but it is delayed by 4–5 months from the precipitation cycle because this basin is fed mostly by snowmelt (Cayan and Peterson 1989; Cayan 1996). During winter there is more than a tenfold range between the 25th and 90th daily precipitation percentiles. Although the lag between precipitation and stream flow takes various time lags over the many basins draining the complex terrain of the western United States (Cayan and Peterson 1989), the delay exhibited by the annual peak of the Merced River flow relative to that of the precipitation illustrates the reason why analyses herein employ precipitation during October–April and a lagged set of stream flow during January–July.

To determine the influence of ENSO upon the frequency of daily precipitation amounts and daily stream flow volume at a given site, the number of days exceeding a prescribed threshold was counted separately for all SOI− cases and for all SOI+ cases. These counts were converted to frequency by dividing by the total number of days (October–April only) in the El Niño and La Niña winters, respectively. In this paper two thresholds, the 50th and the 90th percentiles, are emphasized. In addition, to portray differences between the two ENSO phases, ratios of the frequency of occurrences were obtained by dividing the frequency of occurrence for SOI− cases (designated as f_E, El Niño phase) by that for SOI+ cases (designated as f_L, La Niña phase).

b. Significance tests

A Monte Carlo approach was employed to assess significance of population differences. Precipitation and stream flow records were shuffled and the ''chance'' frequency of occurrence of daily events of median and greater, and 90th percentile and greater, for each of three categories SOI−, SOI+, and neutral, was calculated. This exercise was repeated another 999 times, and frequencies were calculated each time. The shuffle preserved the actual sequence of daily values in the observed record; only the identification of whether a given year was SOI−, SOI+, or neutral was changed. For each synthetic set of years, the observed number of SOI− years (15), SOI+ years (10), and neutral years (23) was preserved. For each station, the likelihood that the frequency of precipitation events for SOI−, SOI+, neutral, and the ratio of SOI− to SOI+, was different than chance occurrence was measured by determining the relative position of the observed frequency within

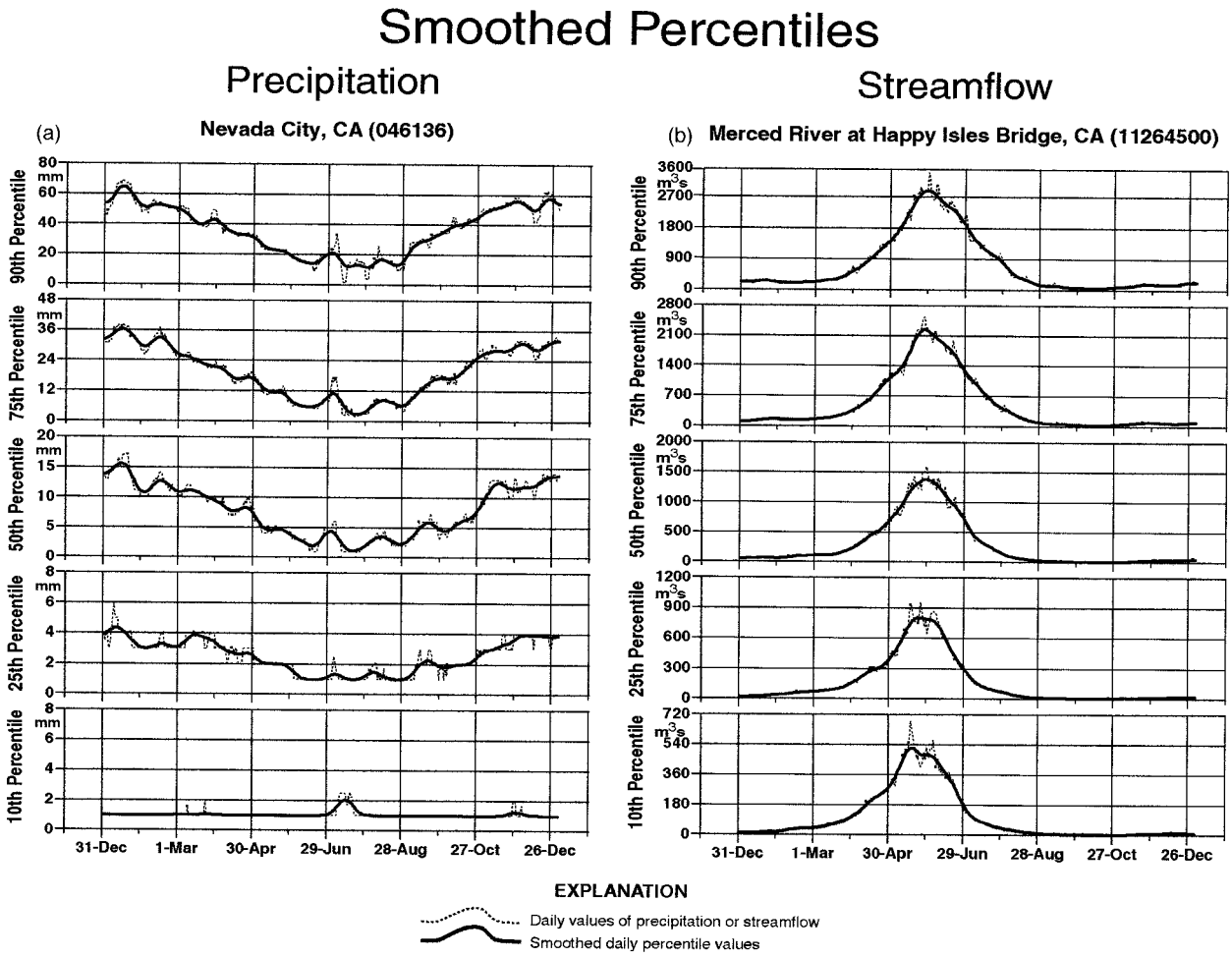

FIG. 4. Smoothed percentiles of (a) daily precipitation, Nevada City, CA, and (b) nearby daily stream flow on the Merced River at Happy Isles Bridge, CA, based on 1948–95 data.

the stack of 1000 frequencies from the Monte Carlo trials. Stations whose significance levels exceed the 90% level of confidence are contoured on the maps presented below.

The determination that a given pattern of precipitation or stream flow frequency was significantly different from chance occurrence also was made using a field significance test (Livezey and Chen 1983) that employed the same Monte Carlo trials as described above but assessed the *number* of stations whose daily precipitation or stream flow frequency exceeded a given threshold, instead of testing an individual station's behavior. In this case, the number of stations with frequency or SOI−/SOI+ frequency ratio greater than its 95th percentile or less than its 5th percentile was tallied for each of the Monte Carlo trials, as well as for the observed set of stations over the western United States. The rank of the number of ''significant'' stations in the observed set, with respect to the stack of such numbers from the Monte Carlo set, was taken to measure the pattern significance.

For several of the analyses presented, the ''seasons'' considered are October–April for precipitation and January–July for stream flow. The stream flow season is lagged with respect to precipitation to allow for the time delay of runoff due to snowpack and other hydrologic storage effects. This set of months is sufficiently broad to describe the ENSO effects on the overall wet season precipitation and resultant stream flow response.

4. Results

a. Individual sites

The frequency distribution of daily precipitation amounts (greater than zero) for October–April during SOI− and SOI+ years is graphed in Fig. 5 for representative sites in the Northwest and Southwest. These plots reflect the opposing tendencies for locations in the Northwest to be drier during SOI− years and wetter in SOI+ years, and vice versa for locations in the Southwest. At both sites, the frequency of light amounts of

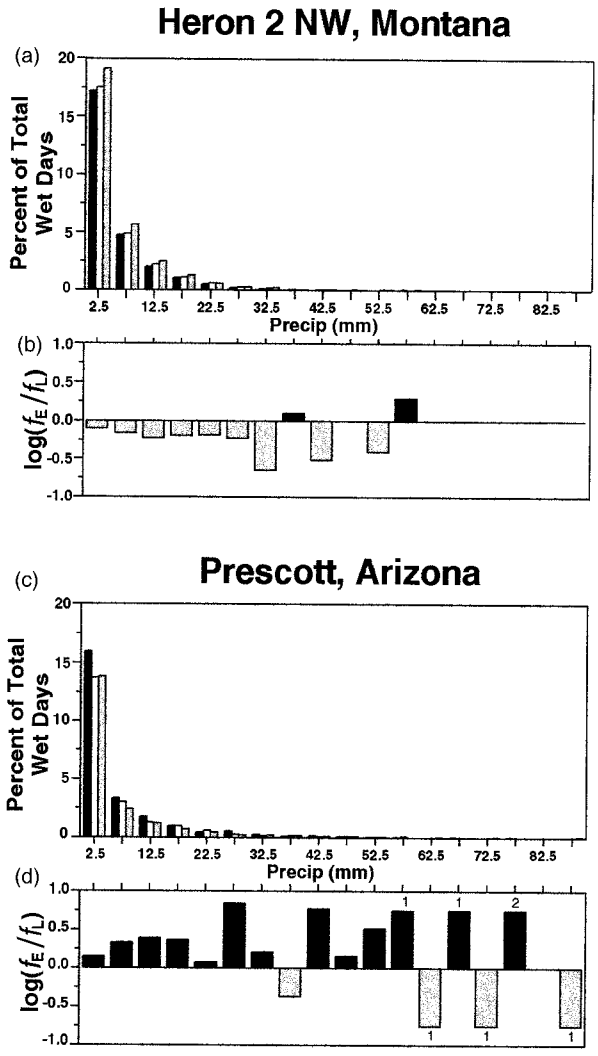

FIG. 5. Frequency distribution of daily precipitation for SOI− years (black bars), neutral years (white bars), and SOI+ years (gray bars) for (a) Heron, MT, and (c) for Prescott, AZ. Sum of frequency values equals fraction of total days that are wet (nonzero precipitation). Based on the period Oct–Apr, 1933–97. (b) and (c) Graph of each pair shows ratio of frequency, SOI−/SOI+; when ratio is infinite (one category has no occurrences), the value plotted is ±0.75, and the number of occurrences in the other category is labeled at top of bar.

daily precipitation (less than 7 mm) is not so different for SOI− and SOI+ years. However, the difference in daily precipitation frequency becomes significant for amounts above 10 mm, and the SOI− versus SOI+ difference in precipitation frequency becomes more disparate with greater precipitation amounts. For example, at Prescott, Arizona (Fig. 5d), the frequency of daily precipitation during SOI− (black bars) is more than three times greater than that during SOI+ (gray bars) for amounts exceeding 20 mm. Many stations in the Southwest exhibit this same tendency for the wettest days to exhibit the largest relative differences in frequency. These results are consistent with those of Woolhiser et al. (1993), who showed that in the Southwest, during the winter months with negative SOI, there were more days with precipitation and more precipitation per day on days with precipitation. Alternatively, in the Northwest, as shown for Heron, Montana (Fig. 5, upper), the same tendency occurs but in the opposite sense, so that the heavier precipitation events are more frequent during SOI+ years and less frequent in SOI− years. Thus, in both regions, the two phases of ENSO appear to oppositely affect the frequency of precipitation, especially for the more intense categories of daily precipitation.

This SOI− versus SOI+ contrast is also found for daily stream flow occurrences. The frequency distributions of daily mean stream flow values during SOI− and SOI+ years were obtained for representative gauge records in the Northwest and in the Southwest. Stream flow differs from precipitation in that there are nonzero flows almost every day (except in arid locations). Thus, increases in one part of the frequency distribution must be balanced by decreases elsewhere in the distribution. In the Southwest, as represented by the Little Colorado River (Fig. 6d), the frequency of high flows is sharply increased during SOI− (black bars) and is decreased during SOI+ (gray bars). It is noteworthy that there are very few flows above 1000 $m^3 s^{-1}$ during SOI+ years. In conjunction, the frequency of very low flows in the Little Colorado increases during SOI+ and decreases during SOI−. In the Northwest, the opposite pattern occurs, as would be expected from the results of the precipitation analysis (discussed above). For example, at Clarks Fork of the Yellowstone River (Fig. 6a,b) the frequency of the high flows is increased during SOI+ (gray bars) and decreased during SOI− (black bars). This tendency is particularly striking for flows above 5000 $m^3 s^{-1}$, so that for the very highest flows, there are no occurrences during SOI− years.

It is not surprising that the response of large daily stream flow events to ENSO is similar to that of heavy precipitation events. However, distributions at the individual sites in Figs. 5 and 6 further suggest that the stream flow response to ENSO is amplified over the precipitation response. For example, high flows on the Little Colorado River are 10 times more frequent during SOI− than SOI+, compared to heavy precipitation events (>20 mm) at Prescott that are only three times as frequent (Table 1). To determine the spatial pattern of ENSO responses, similar analyses were also performed on the network of precipitation and stream flow stations covering the western states.

b. Spatial patterns

For all precipitation stations, the frequency of daily precipitation amounts at least equal to the 50th and 90th percentiles (denoted as P50 and P90) was computed for the period October–April for SOI− years and for SOI+ years. Results are presented as the ratio of the frequency

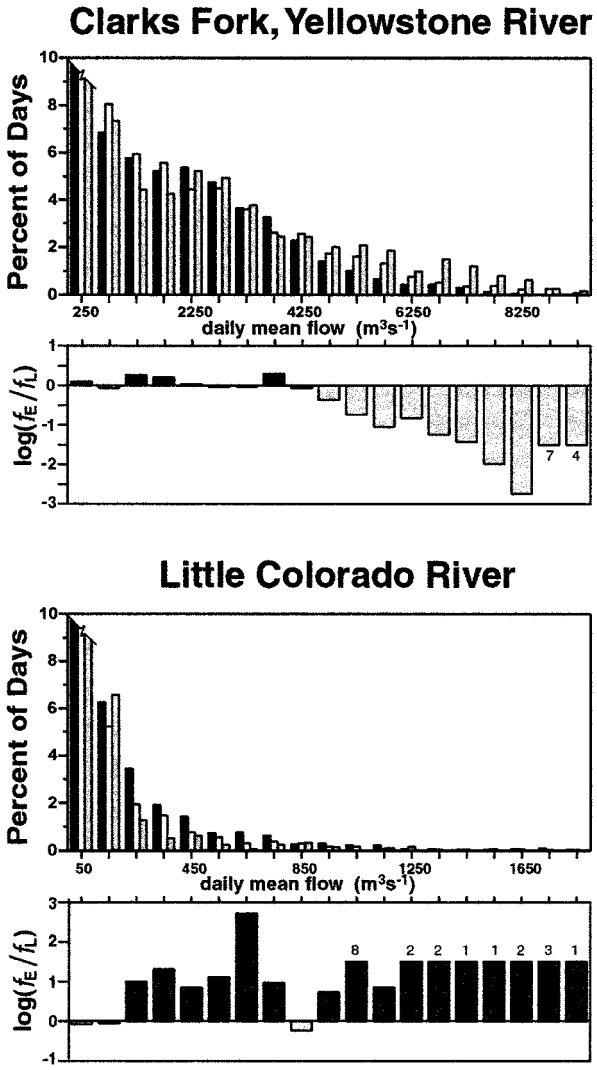

FIG. 6. Frequency distribution of daily mean stream flow for SOI− and SOI+ for (a) Clark's Fork River of the Yellowstone River, near Belfry, MT, and (c) for the Little Colorado River above Lyman Lake, AZ. Based on Jan–Jul, 1948–95, the lowest category of flow in (a) and (c) is truncated in order to display higher flow categories. (b) and (c) Graph of each pair shows ratio of frequency, SOI−/SOI+; when ratio is infinite (one category has no occurrences), the value plotted is 1.5, and the number of occurrences in the other category is labeled at top of bar.

for SOI− years to the frequency for SOI+ years. Statistical significance of the frequency ratios was determined by Monte Carlo resampling of the time series, described in section 3, and is contoured on the maps displaying the frequency ratios. For daily precipitation events exceeding the median, the pattern that emerges (Fig. 7a) is very similar to that described in previous studies (e.g., Redmond and Koch 1991) of the influence of ENSO upon the seasonal mean precipitation. Relative to SOI+ years, SOI− years favor more frequent P50 events in the Southwest and less frequent (only slightly) P50 events in the Northwest. In the Southwest, the ENSO precipitation frequency signal has a higher amplitude than that in the Northwest. Perhaps this is because the absolute frequency values are climatologically lower in the Southwest, so that modest changes in frequency produce a relatively large change between the SOI− and SOI+ states. As will be shown below, to a reasonable approximation, the two phases are opposite in their patterns. The region of increased SOI−/SOI+ ratios extends from southern California eastward through New Mexico, including southern Nevada and southern Utah. The region of decreased SOI−/SOI+ ratios includes parts of Oregon, Washington, most of Idaho, western Montana, and northwest Wyoming. At their strongest core areas, P50 events in the Southwest during SOI− winters are three times more likely than during SOI+ events and are about 70% as likely in the Northwest. The significance calculation indicates that the confidence values in the core region of high SOI−/SOI+ ratios in the Southwest and low ratios in the Northwest rise above the 90% confidence level. The patterns shown on the maps in Fig. 7 and others below are highly significant (>99.9% confidence level), as determined from the field significance test. In none of these tests (1000 trials each) was there a synthetic map that contained significant SOI−/SOI+ frequency ratios over as extensive a portion of the domain as did the map from the real observed daily data.

The P90 precipitation SOI−/SOI+ frequency ratios have a very similar pattern to that of P50 (Fig. 7b), but it is considerably amplified. The area enclosed by the 90% confidence level estimates (dashed line) is very similar to the areas of highest and lowest ratios. Core areas of high and low ratios of SOI−/SOI+ P90 frequencies are in the same locations as for P50 events, but they have expanded, and now the peak ratios exceed 3.5 or are less than 0.5. Regions of highest P90 frequency ratios include southern California, southern Nevada, southern Colorado, Arizona, and western New Mexico. Regions of lowest P90 frequency ratios include the mountainous parts of Oregon and Washington, most of Idaho, western Montana, and the southwest corner of Wyoming.

For stream flow, P50 SOI−/SOI+ frequency ratios (Fig. 7c) have a similar pattern to that for the precipitation, with SOI− years tending to increase the frequency of median and higher flow days in the Southwest and to decrease their frequency in the Northwest, relative to SOI+ years. Interestingly, whereas the precipitation ENSO signal was weaker in the Northwest than in the Southwest, for stream flow the two regions have ratios of more nearly the same strength but in the expected opposite sense. Significance estimates exceeding the 90% confidence level are present in core regions in both the Southwest and Northwest. The similarity of the daily stream flow frequency pattern to that of daily precipitation probably reflects the cause–effect relationship between precipitation and stream flow.

The boldest pattern provided by this set of analyses

TABLE 1. Persistence characteristics of daily precipitation at two representative sites. P1 is the frequency of 1-day precipitation events exceeding the threshold. P11 is the frequency of 2-day precipitation events where both days exceed the threshold. P111 is the frequency of 3-day precipitation events where each day exceeds the threshold. Event categories are unconditional, for example, they do not consider ppt the day before or after the 1-, 2-, or 3-day event. Compiled from daily precipitation data, Oct–Apr 1933–97.

	Heron, Montana (threshold = 6.35 mm) ENSO phase			Prescott, Arizona (threshold = 2.54 mm) ENSO phase		
Event Category:	SOI−	Neutral	SOI+	SOI−	Neutral	SOI+
P1	0.145	0.173	0.190	0.120	0.090	0.078
P11	0.048	0.058	0.066	0.043	0.027	0.019
P111	0.016	0.021	0.029	0.015	0.007	0.007
Days with ppt > threshold	599	1015	483	502	534	198
Total days	4119	5851	2545	4192	5915	2548
Ppt amount (mm day^{-1}) (for all days with ppt > 0)	5.72	6.22	6.50	7.19	7.05	5.64

is the P90 stream flow map (Fig. 7d). The P90 SOI−/SOI+ frequency ratio map has the same pattern as that for the stream flow P50 ratio, but the amplitude is much stronger, and the area enclosed by the 90% confidence level estimates (dashed line) is also expanded. Several stream gauges in the Southwest have P90 SOI−/SOI+ stream flow ratios exceeding 10, and a few exceed 50. Core regions in the Southwest and Northwest have considerable areas with ratios exceeding 15 or less than 0.3. Moreover, the high stream flow P90 ratios extend northward along the West Coast into northern California. Closer inspection shows that the high SOI−/SOI+ ratios in northern California are limited to near-coastal watersheds and do not include watersheds draining the high-elevation Sierra Nevada region. Thus, during warm tropical Pacific (SOI−) years, high flow events in the Southwest occur much more frequently than during cool tropical Pacific years.

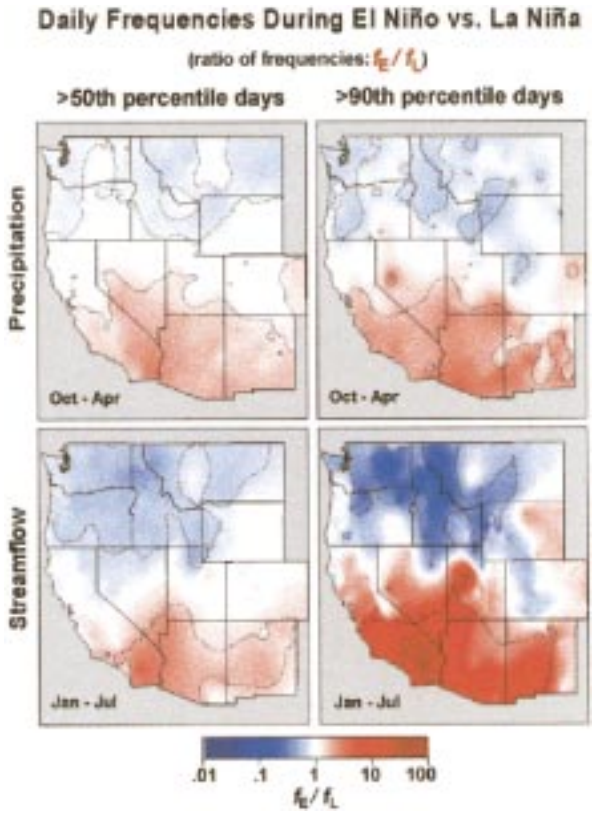

FIG. 7. (a) and (b) Precipitation and (c) and (d) stream flow f_E/f_L ratio of frequencies (SOI−/SOI+) of daily values exceeding (a) and (c) 50th percentile and (b) and (d) 90th percentile. Precipitation during Oct–Apr, stream flow during Jan–Jul, 1948–95. Red denotes ratios >1.0 (SOI− cases have more frequent events than SOI+ cases), blue denotes ratios <1.0 (SOI− cases have less frequent events than SOI+ cases). Dashed lines denote regions where frequency ratio exceeds 90% confidence levels via Monte Carlo trials.

To separate the SOI+ from SOI− frequencies of precipitation and stream flow events, frequency ratios were also calculated for SOI−/neutral cases and SOI+/neutral cases. The frequencies of P90 events reveal the essence of the SOI− and SOI+ behavior and are mapped in the four panels of Fig. 8. The primary conclusion of this analysis is that, for the larger spatial scales, there are approximately opposite patterns of hydrologic extremes over the western United States for the warm and cool phases of ENSO. However, there appear to be some interesting complications to this simple description. Hoerling et al. (1997) show that nonlinearities exist so that the two phases of ENSO do not produce entirely symmetric circulations and attendant surface anomaly patterns.

As might be expected, for the SOI− (El Niño) phase, the maps (Figs. 8b,d) exhibit an increased frequency of extreme (P90) precipitation and stream flow events in the Southwest and decreased frequency in the Northwest. The area of enhanced precipitation and stream flow frequency covers much of California, Nevada, and Arizona, and also fringes along southern Oregon, southern Utah, southwestern Colorado, and parts of New Mexico. Somewhat surprising are quite strong increases in frequency of SOI-stream flow in northern California. Conversely, diminished frequency of high precipitation and streamflow events are found in Washington, northern Oregon, Idaho, and most of Montana. There is also a prominent extension of diminished SOI− frequencies southward into northern Utah and western Colorado, roughly following the Rocky Mountains.

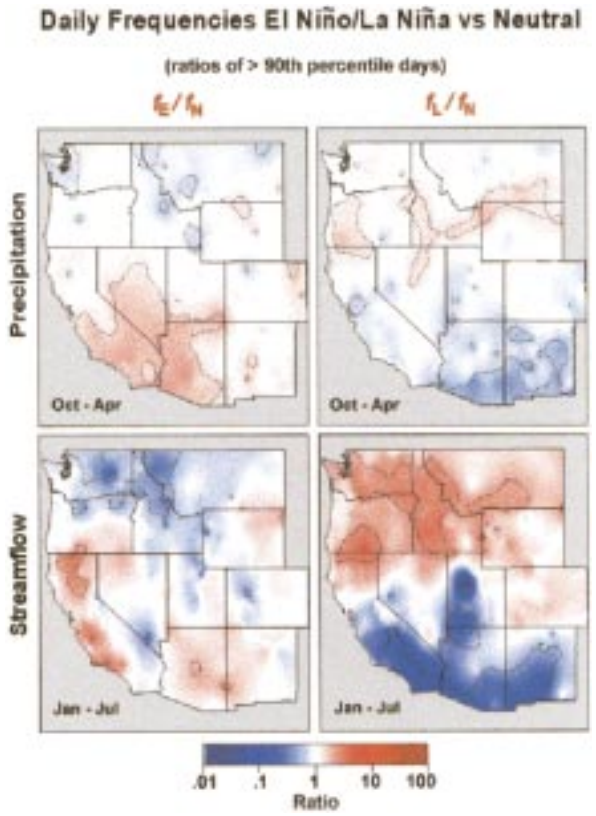

FIG. 8. (a) and (b) Precipitation and (c) and (d) stream flow ratio of frequencies of daily values exceeding 90th percentile, (a) and (c) f_E/f_N, SOI−/neutral and (b) and (d) f_L/f_N, SOI+/neutral. Red denotes ratios >1.0, blue denotes ratios <1.0. Dashed lines denote regions where frequency ratio exceeds 90% of confidence level via Monte Carlo trials.

Noteworthy features of the SOI+/neutral maps (Figs. 8a,c) are that they are nearly the opposite pattern but somewhat stronger than the SOI−/neutral maps. Overall, the El Niño response from this particular dataset is not quite as consistent as the La Niña response. Decreased SOI+/neutral P90 frequency ratios for both precipitation and stream flow are found from California (south of Ukiah) eastward to New Mexico, including southern Nevada and southern Utah. The area of increased frequency ratios during SOI+ includes most of Washington and Oregon, Idaho, and parts of western Montana and western Wyoming. Hoerling et al. (1997) and Livezey et al. (1997) note the lack of symmetry and the variability across ENSO events in more detail. Gershunov and Barnett (1998) and Gershunov (1998) also find nonlinearities in ENSO-related interseasonal precipitation and especially temperature statistics.

As was seen above for the SOI−/SOI+ cases, the SOI−/neutral and SOI+/neutral ratio patterns for stream flow are amplified versions of those for precipitation. The SOI+/neutral stream flow pattern (Fig. 8d) is particularly distinct, with strong core areas in both the Northwest and the Southwest. Hoerling et al. (1997) argue that the existence of thresholds for deep convection provides a thermodynamic pathway for nonlinearity in teleconnected responses. From this, one could infer that differences in ocean temperature patterns among different El Niños might produce more variability in midlatitude response for El Niño than for La Niña. Observations clearly show much more individuality among El Niño responses in the west than among La Niña responses, especially in the Southwest (e.g., Redmond and Koch 1991; Gershunov 1998). Kumar and Hoerling (1997) conclude that internal variability arising from other non-ENSO components of the climate system are likely contributors that provide additional variations between ENSO events.

c. Consistency of ENSO signal

An important aspect of a particular ENSO-related anomaly signal at a given location is how repeatable it is across different ENSO cases. One criterion employed by Ropelewski and Halpert (1986) and later by Kahya and Dracup (1994) in determining whether a particular region contains a reliable ENSO signal was that the number of El Niño events exhibiting the signal must be a large fraction of the total number of such events. Our analyses have only considered an overall lumped population of daily events during all SOI− and all SOI+ cases. To address consistencies within each of the two ENSO phases, the *number of years* with significantly increased or decreased occurrences of extreme October–April daily precipitation and January–July daily stream flow events was tallied. To place a significance estimate upon this ENSO influence at a given station, tercile boundaries of the N90 distribution were computed for neutral year cases, where N90 is the number of days in a given year with precipitation or stream flow exceeding the P90 threshold. Using these, we then determined the fraction of SOI− years and SOI+ years whose P90 count exceeded the upper tercile of neutral year N90 or whose P90 count was less than the lower tercile of neutral year N90. The reliability measure, as displayed, is the difference in percent of the fraction of SOI− or SOI+ years in a given category minus the same fraction for neutral years. Figures 9 (precipitation) and 10 (stream flow) show four measures of the ENSO consistency for each of the two variables: the fraction of SOI− years with unusually (a) high and (b) low N90, and fraction of SOI+ years with unusually (a) high and (b) low N90.

It is pertinent that Fig. 9 contains both SOI− (El Niño) and SOI+ (La Niña) signals, with those for SOI+ being at least as strong as those for SOI−. Equally informative is that areas with anomalously diminished N90 tend to be opposite of those with unusually large N90. For some users, anticipating a diminished number of large precipitation or flow events may be as important as anticipating an increased number, and it would be very useful to know if such a tendency reverses as the

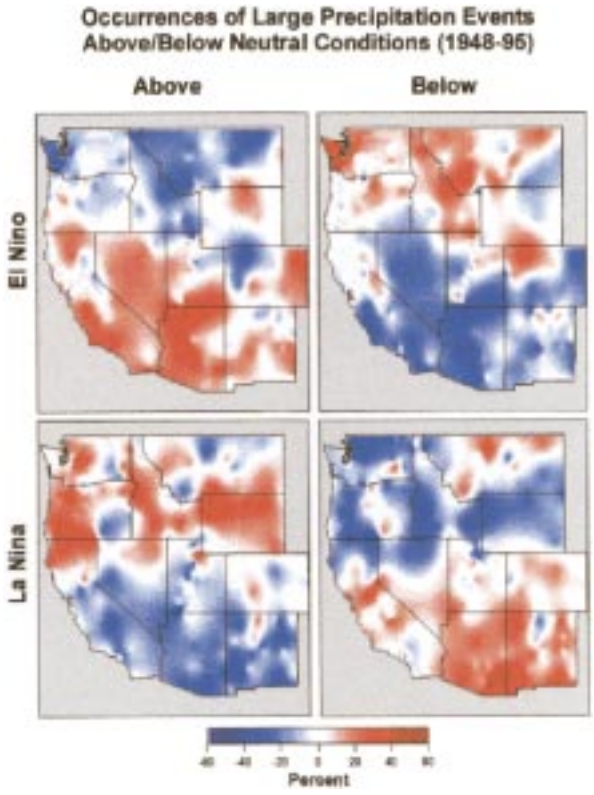

FIG. 9. Differences in fraction of years within category of daily P90 precipitation above/below expected from tercile boundaries of neutral year cases. (a) and (b) SOI− (El Niño) minus neutral and (c) and (d) SOI+ (La Niña) minus neutral. Values are the difference in percent of total years having above expected or below expected number of P90 events.

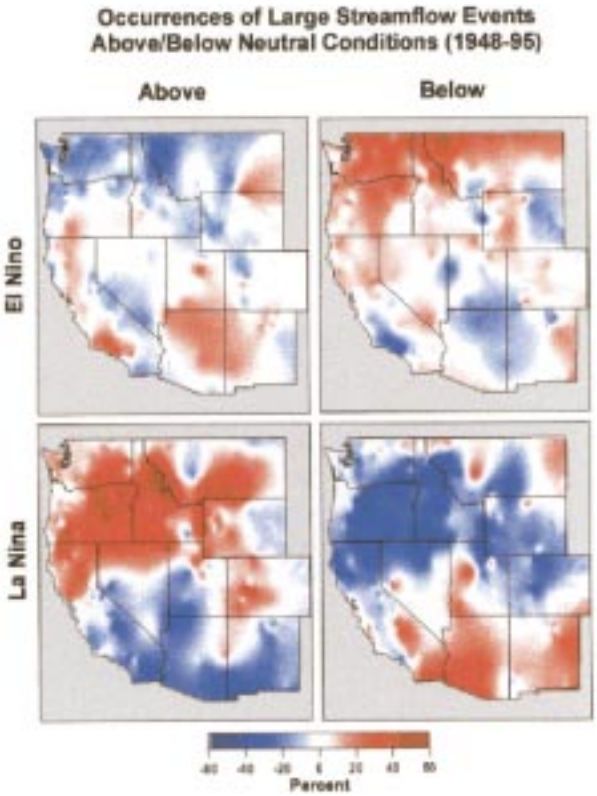

FIG. 10. Differences in fraction of years within category of daily P90 stream flow above/below expected from tercile boundries of neutral year cases. (a) and (b) SOI− (El Niño) minus neutral and (c) and (d) SOI+ (La Niña) minus neutral. Values are the difference in percent of total years having above expected or below expected number of P90 events.

tropical Pacific changes from its warm (SOI−) to its cool (SOI+) phase. In fact, precipitation and stream flow maps are very compatible in showing similar regions and intensities of excessive positive or negative fractions of N90. These ''reliability'' maps also resemble the maps constructed for the lumped population P90 frequencies. Most areas with marked P90 frequencies have a reliable year-to-year consistency of anomalous N90 over the set of SOI− or SOI+ years. In only a few locations do we find that an extraordinary number of daily events during a few ENSO years have biased the P90 frequency of the overall SOI− or SOI+ population. On the high end, this reliability measure exceeds 35% above the upper tercile of N90, and on the low end, this measure is more than 20% below the lower tercile of N90. This reliability measure shows many areas with values of 35%–40% (natural limit is 67%) on both the positive and negative ends of the distributions, indicating that given a certain ENSO phase, there is a high likelihood of winter event counts being in one of the extreme terciles, and a similarly low likelihood of being in the opposing tercile. (Complete symmetry is not required, depending on the number in the middle tercile.) Adopting the reasoning often employed by users of this information, one may think of the reliability issue in terms of forming ''rules'' about climate behavior (i.e., that ENSO state ''x'' brings about climate state ''y'') and how often one would expect such rules to be violated or upheld.

The reliability patterns exhibited by stream flow (Fig. 10) are very similar to those exhibited by precipitation (Fig. 9). Although the amplitude of the difference (or ratio) of frequency of daily events was enhanced for stream flow relative to precipitation (Fig. 5), the reliability of stream flow is not accentuated over that of precipitation. In other words, the number of years with an inordinate number of stream flow events during an SOI− or an SOI+ year is generally no greater than that associated with precipitation events (Fig. 10). That is, if an ENSO year fails to produce an unusually high (or low) number of heavy precipitation daily events, it will also probably fail to achieve an unusually high or low number of stream flow events.

d. Persistence of precipitation events

Because the SOI− versus SOI+ contrast in frequency of high stream flow events is more accentuated than that

for precipitation, it is clear that the hydrologic system is amplifying the effects of meteorological forcing. Aside from simply reflecting a change in frequency of high daily precipitation events, it is possible that ENSO alters other characteristics of precipitation, such as duration Redmond and Cayan (1999), and thus helps to generate higher (or lower) stream flow through the nonlinear response of runoff to precipitation by affecting soil saturation.

This possibility was investigated in a preliminary way by considering two sites representative of the ENSO response core areas. Heron, Montana, is in the interior Northwest, and Prescott, Arizona, is in the west-central part of Arizona, the core of the ENSO response. As a measure of significant precipitation activity, a census was conducted of successive days during October through April in which precipitation was above a specified amount (6.35 mm day^{-1} at Heron and 2.54 mm day^{-1} at Prescott). These were counted by duration (number of one-day events, number of two-day events, and so on), separately for SOI−, SOI+, and neutral years.

In the Southwest (Prescott, Arizona), for both SOI− and SOI+ episodes, the number of occurrences per year falls off markedly from one-day duration events to three-day duration events (Table 1). More pertinently, as duration increases there are considerably more events for SOI− cases than for SOI+ cases, and the proportional difference in number between SOI− and SOI+ cases increases as events become longer. In contrast, in the Northwest (Heron, Montana), there are approximately twice as many three-day precipitation events per year during the SOI+ phases as there are during the SOI− phases; there is one four-day precipitation event in the record for SOI+, and none for SOI−.

Thus, ENSO modifies the duration of precipitation events as well as their frequency and magnitude. In the Southwest, SOI− (El Niño) produces longer-duration precipitation events and SOI+ (La Niñas) produces shorter-duration cases. Conversely, in the Northwest, the opposite behavior is observed. Taken together, these changes in the duration of heavy precipitation storm events help to explain the amplification of the ENSO stream flow signal over its corresponding precipitation signal as well as its pattern over the West. This issue will require further study.

5. Conclusions

An examination of daily historical data over the western United States reveals that the ENSO phase affects the frequency of daily precipitation events. Furthermore, the amount of precipitation on a wet day is changed. In particular, the phase of ENSO shifts the character of precipitation-bearing systems so as to increase or decrease the frequency of larger precipitation events. Further, the frequency of high stream flow events over the region is consistent with that of precipitation. During the cool season coinciding with the mature phase of SOI− events (El Niño, warm tropical Pacific), there is an increase in the frequency of days with high precipitation and stream flow in the Southwest and a decrease in the frequency of days with high precipitation and flows in the Northwest. Nearly the opposite pattern is associated with SOI+ (La Niña, cool tropical Pacific) episodes. This opposition pattern is also evident in results of a recent study by Gershunov and Barnett (1998) of ENSO affects on the frequency and amount of precipitation at stations across the United States. The pattern of SOI− versus that of SOI+ frequency differences relative to the background climatology is roughly symmetric.

Spatial patterns exhibited by the extreme daily precipitation and stream flow tendencies are largely consistent with previous studies that considered the behavior of seasonal total or average quantities, but there are a few surprises. In coastal-central California, ENSO does not appear to influence the frequency of low to modest daily precipitation events. The region does, however, appear to experience an increase in the number of unusually high precipitation and stream flow days during the negative SOI (warm tropical Pacific) cases. This El Niño–enhanced region does not include the Sierra Nevada but extends only about 100 km inland. This potential for differences between the California coastal region and the nearby Sierra Nevada in their response to the two phases of ENSO has important implications for flood risk. Major floods in the Sierra Nevada appear to be more likely during La Niña than during El Niño, whereas major floods in the coastal plain and coast range are more associated with El Niño. Assessment of the nature of the Sierra Nevada–dominated flood threat is critical to protecting lower-lying urban areas in the central valley of California, such as Sacramento. This information may heavily impact which combination of dam construction, levee improvements, altered reservoir strategies, floodplain policies, and behavioral inducements should be selected, and is thus at the center of a contentious, long-standing, and still unresolved public debate.

An important aspect of the hydrologic response to ENSO is that the effect on stream flow is amplified over that of precipitation. Several basins in the Southwest are at least 10 times as likely to experience extremely high flows during SOI− years as during SOI+ years. Also, the stream flow signal persists beyond the active winter precipitation season in the West because of snowmelt lags. Redmond and Koch (1991) point out also that ENSO temperature responses in the two core regions tend to reinforce the precipitation effects on snow accumulation and eventual runoff. During the warm phase of ENSO, the Pacific Northwest has dry and warm winters, and the Southwest has wet and cool winters. Temperature affects the rain/snow elevation, the length of the snowpack accumulation season, and the timing and duration of the melt season. The amplification of the

stream flow signal probably occurs because of an anomalous buildup of soil moisture and its attendant nonlinear influence on runoff, so that wet soils generate considerably more discharge per unit of precipitation than do dry soils. Also, the ENSO-related patterns appear to produce differences in soil moisture conditions related to the duration of precipitating weather systems. During SOI− (El Niño) years, the occurrence of two-day and three-day-in-succession precipitation events is increased in the Southwest (by as much as twice as frequent as during neutral and SOI+ years) and decreased in the Northwest (to nearly half of the occurrence during SOI+ years).

Not all ENSO events are alike, and the hydrologic response differs from one event to another. It is likely that the ''signal'' imposed by great El Niños like 1982/83 and 1997/98 is stronger and somewhat distinct from those of more modest tropical warm events (Hoerling et al. 1997). Nonetheless, even when they are all lumped together, a significant fraction of events, SOI− and SOI+, exhibit accentuated (positive or negative) numbers of extreme events. Judging from the record of daily events available during ENSOs between 1948 and 1995, there is an increased likelihood of accentuated numbers of extreme events by ±30% over neutral years. This offers hope for prediction seasons in advance (see also Gersunov 1998).

These changes in precipitation frequency and amount on daily timescales over large coherent regions is evidence that synoptic-scale patterns (storm tracks, storm intensity, and duration) are modified by the phase of ENSO (Redmond and Cayan 1999). SOI− winters favor low-latitude storm tracks and possibly an enhanced moisture source across the North Pacific, while SOI+ events are conducive to higher-latitude systems.

In this paper we have explored the connection of hydrologic extremes to ENSO using a very simple measure, the two-barometer Tahiti-minus-Darwin Southern Oscillation index averaged over June–November. The results indicate that the state of ENSO in the tropical Pacific during summer–fall provides a look ahead into the likelihood of extreme daily precipitation and stream flow events over several subsequent seasons. Furthermore, it offers a route to practical utilization by water managers in anticipating increased (or decreased) risk of flooding and in forecasting spring–summer water supplies. These are issues of critical concern in the West, where recent decades have seen remarkable interannual climate fluctuations, and where water supplies and water quality are increasingly stressed. Also, implications for other regions are encouraging; because of the similarity in positively skewed rainfall and flow distributions around the globe, this approach may be used to forecast extremes in other regions having ENSO signals in monthly or seasonal precipitation.

Acknowledgments. Nicki Pyles provided word processing and editorial help. Updates of the USGS stream flow data were provided by Mike Dettinger, and time series of NOAA weather data were provided by Jim Ashby of the Western Regional Climate Center. We thank Mike Dettinger and Alexander Gershunov and two anonymous reviewers for valuable discussions and careful review of the manuscript. Funding was provided by the NOAA/Experimental Climate Prediction Center at the Scripps Institution of Oceanography, the Scripps-Lamont Consortium, the California Department of Bontini, and Waterways, and the NSF Climate Dynamics Program, Grant ATM-9509780 (DRC and LGR), the Water Resources Division, U.S. Geological Survey (DRC), and the Western Regional Climate Center (KTR).

REFERENCES

Andrade, E. R., and W. D. Sellers, 1988: El Niño and its effect on precipitation in Arizona. *J. Climatol.,* **8,** 403–410.

Cayan, D. R., 1996: Interannual climate variability and snowpack in the western United States. *J. Climate,* **9,** 928–948.

——, and D. H. Peterson, 1989: The influence of North Pacific circulation on streamflow in the West. *Aspects of Climate Variability in the Pacific and Western Americas, Geophys. Monogr.,* No. 55, Amer. Geophys. Union, 375–398.

——, and R. H. Webb, 1992: El Niño/Southern Oscillation and streamflow in the western U.S. *Historical and Paleoclimatic Aspects of the Southern Oscillation,* H. F. Diaz and V. Markgraf, Eds., Cambridge University Press, 29–68.

Dettinger, M. D., D. R. Cayan, H. F. Diaz, and D. M. Meko, 1998: North–south precipitation patterns in western North America on interannual-to-decadal timescales. *J. Climate,* **11,** 3095–3111.

——, ——, G. J. McCabe, and J. A. Morego, 1999: Multiscale hydrologic variability associated with El Niño/Southern Oscillation. *El Niño–Southern Oscillation: Multiscale Variability and Societal Impacts,* H. F. Diaz and V. Markgraf, Eds., Cambridge University Press, in press.

Dracup, J. A., and E. Kahya, 1994: The relationships between U.S. streamflow and La Niña events. *Water Resour. Res.,* **30,** 2133–2141.

Farnes, P. E., 1995: Estimating monthly distribution of average annual precipitation in mountainous areas of Montana. *Proc. Western Snow Conf.,* Sparks, NV, 78–87.

Gershunov, A., 1998: ENSO influence on intraseasonal extreme rainfall and temperature frequencies in the contiguous United States: Implications for long-range predictability. *J. Climate,* **11,** 3192–3203.

——, and T. P. Barnett, 1998: ENSO influence on intraseasonal extreme rainfall and temperature frequencies in the contiguous United States: Observations and model results. *J. Climate,* **11,** 1575–1586.

Harrison, D. E., and N. K. Larkin, 1998: The El Niño surface temperature and wind anomalies, 1946–1993. *Rev. Geophys.,* **36,** 353–399.

Hoerling, M. P., A. Kumar, and M. Zhong, 1997: El Niño, La Niña, and the nonlinearity of their teleconnections. *J. Climate,* **10,** 1769–1786.

Kahya, E., and J. A. Dracup, 1993: U.S. streamflow patterns in relation to the relation to the El Niño/Southern Oscillation. *Water Resour. Res.,* **29,** 2491–2503.

——, and ——, 1994: The influences of Type 1 El Niño and La Niña events on streamflows in the Pacific Southwest of the United States. *J. Climate,* **7,** 965–976.

Karl, T., and R. Knight, 1998: Secular trends of precipitation amount, frequency, and intensity in the United States. *Bull. Amer. Meteor. Soc.,* **79,** 231–241.

Kiladis, G., and H. F. Diaz, 1989: Global climatic anomalies asso-

ciated with extremes of the Southern Oscillation. *J. Climate,* **2,** 1069–1090.
Kumar, A., and M. P. Hoerling, 1997: Interpretation and implications of the observed inter–El Niño variability. *J. Climate,* **10,** 83–91.
Livezey, R. E., and W. Y. Chen, 1983: Statistical field significance and its determination by Monte Carlo techniques. *Mon. Wea. Rev.,* **111,** 46–59.
——, M. Masutani, A. Leetma, H. Rui, M. Ji, and A. Kumar, 1997: Teleconnective response of the Pacific–North American region atmosphere to large central equatorial Pacific SST anomalies. *J. Climate,* **10,** 1787–1820.
Piechota, T. C., J. A. Dracup, and R. G. Fovell, 1997: Western U.S. streamflow and atmospheric circulation patterns during El Niño–Southern Oscillation. *J. Hydrol.,* **201,** 249–271.
Pulwarty, R. S., and K. T. Redmond, 1997: Climate and salmon restoration in the Columbia River basin: The role and usability of seasonal forecasts. *Bull. Amer. Meteor. Soc.,* **78,** 381–397.
Rasmusson, E. M, and T. H. Carpenter, 1982: Variations in tropical sea surface temperature and surface wind fields associated with the Southern Oscillation/El Niño. *Mon. Wea. Rev.,* **110,** 354–384.
——, and J. M. Wallace, 1983: Meteorological aspects of the El Niño/Southern Oscillation. *Science,* **222,** 1195–1202.
Redmond, K. T., and R. W. Koch, 1991: Surface climate and streamflow variability in the western United States and their relationship to large-scale circulation indices. *Water Resour. Res.,* **27,** 2381–2399.
——, and D. R. Cayan, 1994: El Niño/Southern Oscillation and western climate variability. *Proc. Sixth Conf. on Climate Variations,* Nashville, TN, Amer. Meteor. Soc., 141–145.
——, and ——, 1999: ENSO phase and precipitation persistence in the western U.S. Preprints, *11th Conf. on Applied Climatology,* Dallas, TX, Amer. Meteor. Soc., 309–313.
Ropelewski, C. F., and M. S. Halpert, 1986: North American precipitation and temperature patterns associated with the El Niño/Southern Oscillation (ENSO). *Mon. Wea. Rev.,* **114,** 2352–2362.
——, and P. D. Jones, 1987: An extension of the Tahiti–Darwin Southern Oscillation index. *Mon. Wea. Rev.,* **115,** 2161–2165.
Schonher, T., and S. E. Nicholson, 1989: The relationship between California rainfall and ENSO events. *J. Climate,* **2,** 1258–1269.
Shabbar, A., B. Bonsal, and M. Khandekar, 1997: Canadian precipitation patterns associated with the Southern Oscillation. *J. Climate,* **10,** 3106–3127.
Slack, J. R., and J. M. Landwehr, 1992: Hydro-Climatic Data Network (HCDN): A U.S. Geological Survey streamflow data set for the United States for the study of climate variations, 1874–1988. U.S. Geological Survey Open-File Rep. 92-129, 200 pp. [Available from U.S. Geological Survey, Books and Open File Reports Section, Federal Ctr., Box 25286, Denver, CO 80225.]
Wolter, K., and M. S. Timlin, 1998: Measuring the strength of ENSO—How does 1997/98 rank? *Weather,* **53,** 315–324.
Woodhouse, C. A., and D. Meko, 1997: Number of winter precipitation days reconstructed from southwestern tree rings. *J. Climate,* **10,** 2663–2669.
Woolhiser, D. A., T. O. Keefer, and K. T. Redmond, 1993: Southern Oscillation effects on daily precipitation in the southwestern United States. *Water Resour. Res.,* **29,** 1287–1295.
Yarnall, B., and H. F. Diaz, 1986: Relationships between extremes of the Southern Oscillation and the winter climate of the Anglo-American Pacific coast. *J. Climatol.,* **6,** 197–219.